Molecules and Cells

Oleoylethanolamide Exhibits GPR119-Dependent Inhibition of Osteoclast Function and GPR119-Independent Promotion of Osteoclast Apoptosis

Hyun-Ju Kim*, Dong-Kyo Lee, Xian Jin, Xiangguo Che, and Je-Yong Choi*

Department of Biochemistry and Cell Biology, Cell and Matrix Research Institute, BK21 PLUS KNU Biomedical Convergence Program, School of Medicine, Kyungpook National University, Daegu 41944, Korea
*Correspondence: biohjk@knu.ac.kr (HJK); jechoi@knu.ac.kr (JYC)
https://doi.org/10.14348/molcells.2020.2260
www.molcells.org

Oleoylethanolamide (OEA), a bioactive lipid in bone, is known as an endogenous ligand for G protein-coupled receptor 119 (GPR119). Here, we explored the effects of OEA on osteoclast differentiation, function, and survival. While OEA inhibits osteoclast resorptive function by disrupting actin cytoskeleton, it does not affect receptor activator of nuclear factor-κB ligand (RANKL)-induced osteoclast differentiation. OEA attenuates osteoclast spreading, blocks actin ring formation, and eventually impairs bone resorption. Mechanistically, OEA inhibits Rac activation in response to macrophage colony-stimulating factor (M-CSF), but not RANKL. Furthermore, the OEA-mediated cytoskeletal disorganization is abrogated by GPR119 knockdown using small hairpin RNA (shRNA), indicating that GPR119 is pivotal for osteoclast cytoskeletal organization. In addition, OEA induces apoptosis in both control and GPR119 shRNA-transduced osteoclasts, suggesting that GPR119 is not required for osteoclast apoptosis. Collectively, our findings reveal that OEA has inhibitory effects on osteoclast function and survival of mature osteoclasts via GPR119-dependent and GPR119-independent pathways, respectively.

Keywords: apoptosis, cytoskeleton, G protein-coupled receptor 119, oleoylethanolamide, osteoclast

INTRODUCTION

Osteoclasts, the unique bone-degrading cells, are pivotal to bone remodeling and calcium homeostasis (Boyle et al., 2003; Takayanagi, 2007; Teitelbaum, 2000). These polykaryons are formed by the differentiation and fusion of hematopoietic progenitors of the monocyte-macrophage cell lineage. Two cytokines, receptor activator of nuclear factor-κB ligand (RANKL) and macrophage colony-stimulating factor (M-CSF), are essential for osteoclast formation (Kong et al., 1999; Lacey et al., 1998; Wong et al., 1997; Yasuda et al., 1998). While RANKL primarily triggers osteoclastogenesis, M-CSF promotes precursor cell proliferation and osteoclast survival. Differentiated osteoclasts dramatically reorganize their actin cytoskeleton for bone resorption in response to M-CSF and RANKL. Upon attachment to bone, osteoclasts form a characteristic actin ring or sealing zone, a region that tightly associates the osteoclast and bone matrix surface and separates the resorption area from the extracellular space. The ability of mature osteoclasts to degrade bone matrix is dependent on the formation of the actin ring.

Rho family GTPases play a critical role in regulating various cellular functions, such as actin organization, migration, adhesion, spreading, and microtubule polarization (Chellaiah et al., 2000; Itzstein et al., 2011; Touaitahuata et al., 2014). Post-translational modification by guanine nucleotide-ex-

Received 6 November, 2019; revised 9 December, 2019; accepted 10 December, 2019; published online 13 February, 2020

eISSN: 0219-1032

change factors (GEFs) and GTPase-activating proteins (GAPs) toggles Rho family GTPases between inactive (GDP-bound) and active (GTP-bound) states. Osteoclast cytoskeletal organization depends upon the activity of several Rho GTPases, particularly Rac and Cdc42. The importance of Rho GTPases in osteoclast function has been well-demonstrated using *in vivo* genetic approaches. In osteoclasts or their precursors, deleting Rac, Cdc42, or GEFs results in severe osteopetrosis due to defects in cytoskeletal organization and bone resorption (Croke et al., 2011; Faccio et al., 2005; Ito et al., 2010; Itokowa et al., 2011; Vives et al., 2011).

There is increasing evidence that lipids, including fatty acids and their derivatives, play a key role as signaling molecules in diverse tissues. In skeletal tissue, a targeted lipidomic strategy revealed the occurrence of fatty acid amides (FAA) in bone (Smoum et al., 2010). Among these FAAs, oleoylethanolamide (OEA) has been proposed as an endogenous ligand of G protein-coupled receptor 119 (GPR119) (Overton et al., 2006). GPR119 is abundant in pancreatic beta cells and represents a novel target for treating type 2 diabetes. Furthermore, the administration of synthetic GPR119 agonists reportedly increases bone mineral content and density in a diabetic mouse model (McKillop et al., 2016). Moreover, we recently detected GPR119 in osteoclast lineage cells (Kim et al., 2019b).

OEA is known to decrease body weight and suppress food intake, suggesting the possibility of its involvement in satiety control (Fu et al., 2003; Overton et al., 2006; Provensi et al., 2014; Rodriguez de Fonseca et al., 2001). OEA also promotes the release of glucagon-like peptide-1 with potent insulinotropic effect from the intestinal cells through GPR119 (Lauffer et al., 2009), suggesting that OEA and GPR119 may have potential therapeutic implications in diabetes therapy. OEA, together with other fatty acid ethanolamides, has also been reported to induce cell death in high-grade astrocytoma brain tumors (Stock et al., 2012). Another recent study demonstrated that OEA influences intestinal homeostasis by altering gut microbiota composition (Di Paola et al., 2018). However, the impact of OEA on bone metabolism remains unknown. Furthermore, the relevance of OEA as a physiological ligand of GPR119 to osteoclast development is unclear. Therefore, we explored the effects of OEA on osteoclast differentiation, function, and survival. We also assessed the role of GPR119 in the osteoclast response to OEA by employing GPR119-specific small hairpin RNAs.

MATERIALS AND METHODS

Reagents

OEA was obtained from Tocris Bioscience (USA). Recombinant human M-CSF and mouse RANKL were purchased from R&D Systems (USA). Antibodies against Bim and NFATc1 were purchased from BD Biosciences (USA). Antibodies against phosphorylated-ERK, ERK, and caspase 3 were obtained from Cell Signaling Technology (USA). Lentiviral constructs bearing control and GPR119 shRNA were purchased from Sigma-Aldrich (USA).

Osteoclast culture

Murine osteoclasts were prepared from bone marrow macrophages (BMMs) as previously described (Kim et al., 2019a). Briefly, bone marrow was extracted from the femur and tibia of 8- to 9-week-old mice. The cells were incubated with erythrocyte lysis buffer for 5 min and cultured for 3 days in α-MEM with 10% FBS and 10% CMG 14-12 cell culture medium (Takeshita et al., 2000) containing M-CSF in petri-dishes. The adherent cells were harvested as osteoclast precursors (BMMs). Osteoclasts were generated by culturing BMMs in α-MEM containing 10% FBS, M-CSF (30 ng/ml), and RANKL (30 ng/ml) for 4 to 5 days. Osteoclasts were fixed and subjected to tartrate-resistant acid phosphatase (TRAP) staining.

Reverse transcription polymerase chain reaction (RT-PCR)

RNA was isolated from cells using TRIzol reagent (Invitrogen, USA). cDNA was synthesized from total RNA (1 μg) using a PrimeScript 1st strand cDNA Synthesis Kit (Takara, Japan). RT-PCR was conducted with the following primer sets: GPR119, 5'-CCTCACCGTCATGCTGATTG-3' and 5'-GACCAGGACAGAGTGAAGCT-3'; and GAPDH, 5'-ACTTTGTCAAGCTCATTTCC-3' and 5'-TGCAGCGAACTTTATTGATG-3'.

Quantitative real-time PCR

Real-time PCR analysis was carried out as described (Kim et al., 2019a; 2019c). The sequences of primers were as follows: GPR119, 5'-GCTGATTGCCTTTGACAGATACC-3' and 5'-AAGCCCATTCATGATCTGGAA-3'; TRAP, 5'-TCCCCAATGCCCCATTC-3' and 5'-CGGTTCTGGCGATCTCTTTG-3'; c-Fos, 5'-AGGCCCAGTGGCTCAGAGA-3' and 5'-GCTCCCAGTCTGCTGCATAGA-3'; NFATc1, 5'-ACCACCTTTCCGCAACCA-3' and 5'-TTCCGTTTCCCGTTGCA-3'; Atp6v0d2, 5'-GAGCTGTACTTCAATGTGGACCAT-3' and 5'-CTGGCTTTGCATCCTCGAA-3'; and DC-STAMP, 5'-CTTCCGTGGGCCAGAAGTT-3' and 5'-AGGCCAGTGCTGACTAGGATGA-3'.

Immunoblot analyses

Cultured cells were harvested after washing with cold phosphate-buffered saline (PBS). The cells were then lysed in RIPA buffer (Sigma-Aldrich) containing Halt protease and phosphatase inhibitor cocktail (Thermo Scientific, USA). Protein concentration was determined using a bicinchoninic acid (BCA) protein assay kit (Pierce Biotechnology, USA). Equivalent protein quantities were resolved by 10% or 12% SDS-PAGE and transferred onto PVDF membranes. After blocking in 5% nonfat milk/Tris-buffered saline with 0.1% Tween 20, membranes were subjected to immunoblot analysis. Immunoreactivity was quantified using an ECL-Plus detection kit (Amersham Pharmacia Biotech, USA).

Lentivirus production and infection

Control or GPR119 lentiviral shRNA vector was co-transfected with virus packaging plasmids (ΔH8.2 and VSVG) into HEK293-T cells using the FuGENE HD transfection reagent (Promega, USA). After a 24 to 48 h transfection, virus supernatants were harvested. BMMs were infected with the virus supernatant in the presence of protamine sulfate (10 μg/ml) for 24 h. Infected cells were selected in α-MEM containing puromycin (4 μg/ml) for 2 to 3 days.

Proliferation assay

BMMs were seeded in 96-well plates and incubated for 3 days with M-CSF in the absence or presence of RANKL with OEA at the indicated concentrations. The cells were then incubated with 0.1% BrdU for 4 h. BrdU incorporation was measured by the Cell Proliferation ELISA kit (GE Healthcare, UK).

Apoptosis assay

Mature osteoclasts were generated and then incubated for 24 h with or without OEA. The apoptosis assay was performed using a Cell Death Detection ELISA Plus kit (Roche, Germany) according to the manufacturer's instructions.

Actin ring formation and bone resorption assay

BMMs were seeded on glass slides or bone slices and then

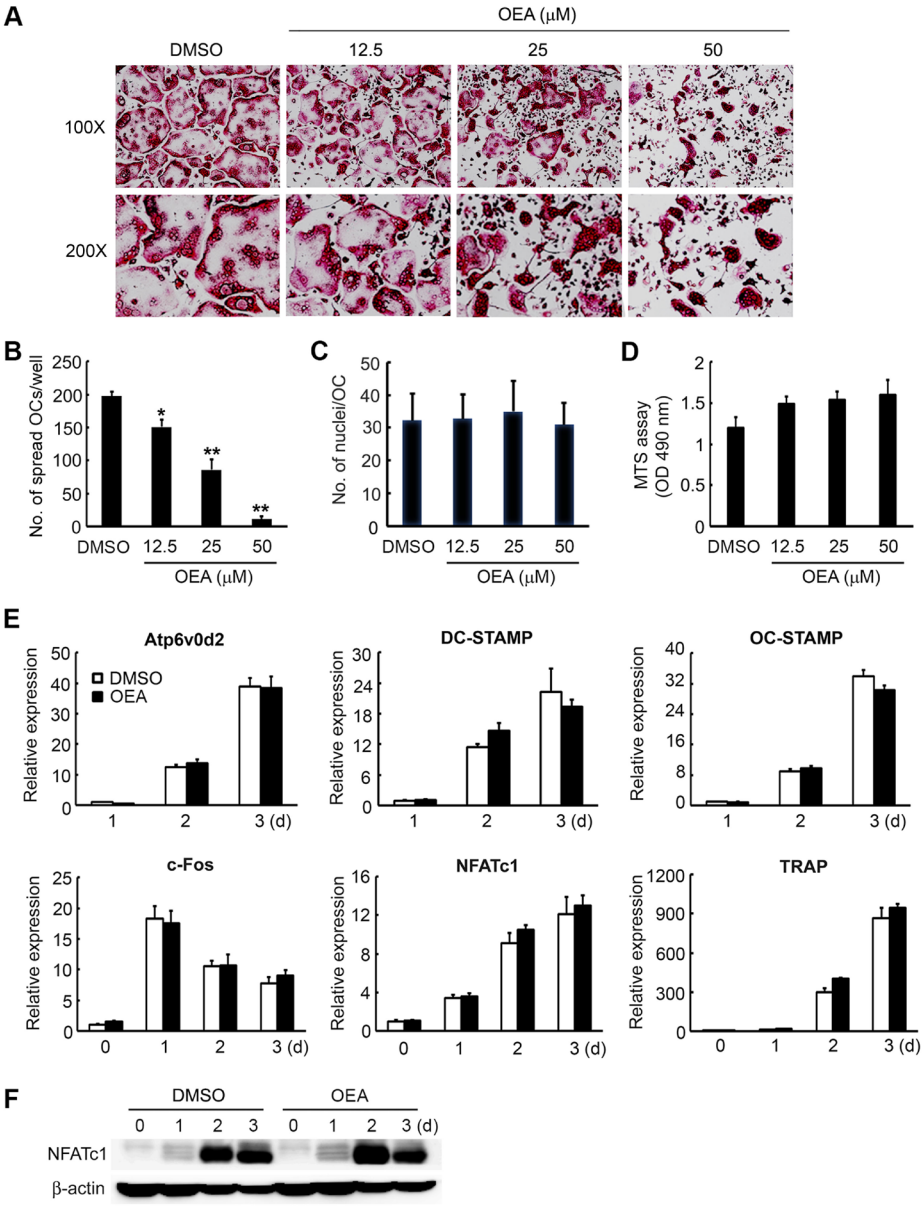

Fig. 1. OEA inhibits osteoclast spreading but not differentiation. (A-C) BMMs were cultured with M-CSF (30 ng/ml) and RANKL (30 ng/ml) for 4 days in the presence of the indicated concentrations of OEA. (A) The cells were fixed and subjected to TRAP staining and observed at 100× (upper panel) and 200× (lower panel) magnifications. (B) Quantification of spread osteoclasts (OCs) per well in Fig. 1A. The data are expressed as the mean ± SD. $*P < 0.05$, $**P < 0.001$ vs the vehicle-treated control (DMSO) cells. (C) The number of nuclei per OC in Fig. 1A was counted. (D) BMMs were cultured at the indicated OEA concentrations in the presence of M-CSF (30 ng/ml). After 3 days, cell viability was determined using the MTS assay. (E and F) BMMs were cultured with OEA (50 μM) or vehicle in osteoclastogenic medium. Real-time PCR (E) or immunoblotting (F) was conducted to detect the expression of osteoclastogenic markers on the indicated days.

cultured with RANKL (30 ng/ml) and M-CSF (30 ng/ml) for 3 days. After 3 days in culture, cells were incubated for an additional 1 to 2 days with or without OEA (50 μM) in osteoclastogenic medium. Cultured cells were fixed with paraformaldehyde, followed by permeabilization in 0.1% Triton X-100/PBS and blocking in 0.2% BSA/PBS. F-actin and nuclei were stained with Alexa Fluor 488 phalloidin (Invitrogen) and Hoechst 33258 (Sigma-Aldrich), respectively. To quantify resorption pits, osteoclasts were removed from bone slices. The bone slices were incubated with horseradish peroxidase-wheat germ agglutinin (WGA) (Sigma-Aldrich) and then stained with 3,3'-diaminobenzidine (Sigma-Aldrich). The area of resorption lacunae was measured by a Java-based image analysis program (ImageJ; National Institutes of Health, USA).

Rac activity assay

Rac activity was determined using an Active Rac1 Pull-Down and Detection Kit (Thermo Scientific). Briefly, cytokine-starved pre-osteoclasts were incubated for 16 h with or without OEA (50 μM). The cells were then exposed to M-CSF (100 ng/ml), RANKL (100 ng/ml), or M-CSF (50 ng/ml) plus RANKL (50 ng/ml) for 20 min. After measuring the protein concentration, cell lysates (1 mg) were subjected to the GST-human-Pak1-PBD pull-down assay. The samples were loaded on a 12% SDS-PAGE and immunoblotted using anti-Rac antibody.

Statistical analyses

Statistical significance was calculated by Student's *t*-test using Microsoft Excel 2016 (Microsoft, USA). $P < 0.05$ is considered to be statistically significant. All data are represented as mean ± SD.

RESULTS

OEA affects osteoclast spreading but not differentiation

To assess the impact of OEA on osteoclasts, we cultured osteoclast precursors (BMMs) with various OEA concentrations or an equivalent volume of DMSO used as the vehicle for OEA in the presence of RANKL (30 ng/ml) and M-CSF (30 ng/ml). Although BMMs exposed to DMSO generate characteristic well-spread osteoclasts, OEA-treated cells are unable to spread, resulting in the formation of small, TRAP-expressing, multinuclear osteoclasts (Fig. 1A). OEA reduces the number of well-spread osteoclasts in a dose-dependent manner and inhibits cell spreading by 95% at 50 μM (Fig. 1B). The small size of OEA-treated cells may indicate that the fusion of TRAP-expressing mononuclear precursors is impaired. To determine if this is the case, we counted the number of nuclei per osteoclast and observed that there is no distinguishable difference between control and OEA-treated cells (Fig. 1C), indicating that OEA does not affect osteoclast fusion. Furthermore, mRNA expression levels of Atp6v0d2, DC-STAMP, and OC-STAMP, which play a critical role in the osteoclast fusion process, remain unchanged in OEA-treated cells (Fig. 1E). We also observed that OEA does not affect BMM viability at any concentration tested (Fig. 1D).

We then investigated OEA influence on RANKL-induced osteoclast differentiation by assessing OEA impact on the expression of osteoclast-specific genes. BMMs were incubated with OEA in osteoclastogenic medium for 3 days. OEA does not affect mRNA expression levels of osteoclastogenesis markers such as c-Fos, NFATc1, and TRAP (Fig. 1E). Consistent with this finding, the protein level of NFATc1, a master regulator of osteoclast differentiation, is comparable between control and OEA-treated cells (Fig. 1F).

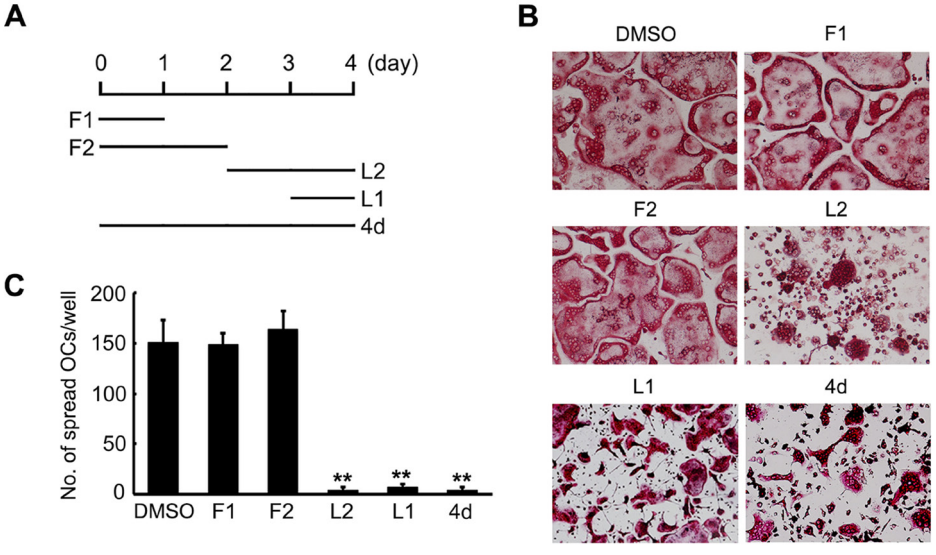

Fig. 2. OEA inhibits cell spreading at the later stage of osteoclast development. BMMs were cultured for 4 days in M-CSF and RANKL. The cells were treated with OEA (50 μM) for the first day (F1), first 2 days (F2), last 2 days (L2), and last day (L1), or the entire 4 days (4d). Control cells (DMSO) were maintained in the absence of OEA for 4 days. (A) Duration of exposure to OEA in days. (B) Osteoclastogenic cultures stained for TRAP activity (magnification, 200×). (C) Statistical analyses of spread osteoclasts (OCs)/well. $**P < 0.001$ vs the vehicle-treated control (DMSO) cells.

OEA blocks cell spreading at the later stage of osteoclast development

The development of osteoclasts is a multistage process comprising proliferation, differentiation, fusion, and maturation, yielding osteoclasts with a well-spread morphology, which is critical for bone degradation. To determine the stage at which OEA inhibits osteoclast spreading, we added OEA to BMMs in osteoclastogenic medium for different culture periods (Fig. 2A). Although adding OEA to BMMs for the first day (F1) or first 2 days (F2) does not affect osteoclast spreading, OEA exposure during the last 2 days (L2) or the last day (L1) of osteoclastogenic culture is sufficient to inhibit cell spreading (Figs. 2B and 2C). These data reveal that OEA effectively blocks osteoclast spreading at the later stage of osteoclast development.

OEA inhibits osteoclast cytoskeletal organization

The OEA-mediated morphological changes in osteoclasts suggest that OEA may influence the organization of actin cytoskeleton. To determine if this is true, we investigated the effect of OEA on the generation of the actin ring, a unique cytoskeletal feature essential for the resorptive activity of mature polykaryons. BMMs were cultured on glass slides in osteoclastogenic medium for 3 days and incubated with OEA or vehicle (DMSO) for an additional day. The actin cytoskeleton was then immunostained with FITC-conjugated phalloidin. Although vehicle-exposed cells reveal typical actin rings, OEA-exposed cells fail to form actin rings from actin clusters

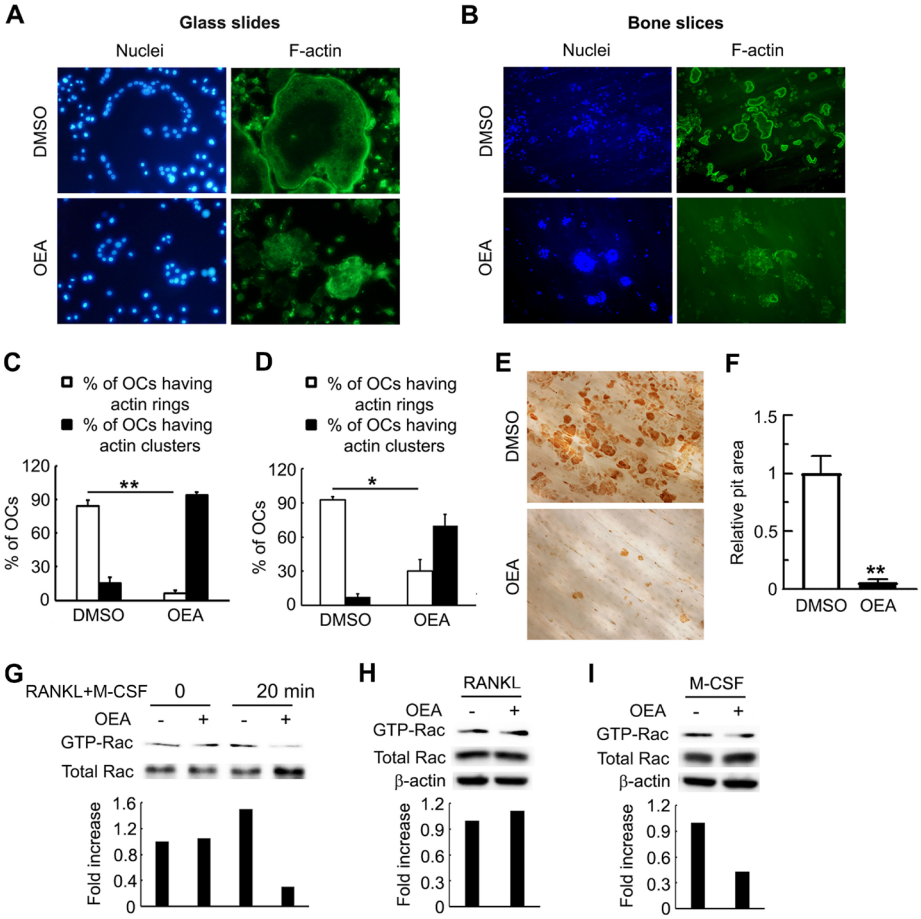

Fig. 3. OEA impairs cytoskeletal organization and bone resorption in osteoclasts. (A and B) BMMs were cultured on glass slides (A) or bone slices (B) for 3 days to commit them to a pre-osteoclast phenotype. The cells were then treated with or without OEA (50 μM) for 1 to 2 days in osteoclastogenic medium. Nuclei and F-actin were stained with Hoechst stain (magnification, 200×; blue) and FITC-conjugated phalloidin (magnification, 200×; green), respectively. (C and D) Quantification of percentage of osteoclasts containing actin rings (white bars) or clusters (black bars) on glass slides (C) or bone slices (D). $*P < 0.05$, $**P < 0.001$. (E and F) BMMs were cultured on bone slices for 3 days with M-CSF and RANKL. The cells were then treated with OEA (50 μM) or vehicle for 2 days in osteoclastogenic medium. (E) Bone slices were stained with peroxidase-conjugated wheat-germ agglutinin (magnification, 100×) after removal of cells. (F) The resorption pit area was measured with an image analysis software. $**P < 0.001$. (G-I) OEA inhibits M-CSF-induced Rac activation. Cytokine-starved pre-osteoclasts were exposed to OEA (50 μM) or vehicle for 16 h. The cells were then stimulated with RANKL (50 ng/ml) plus M-CSF (50 ng/ml) (G), RANKL (100 ng/ml) (H), or M-CSF (100 ng/ml) (I). GTP-Rac was isolated by GST pull-down and immunoblotted with Rac-specific antibody. The fold difference of GTP-Rac levels normalized to total Rac is represented in the bar graphs.

(Figs. 3A and 3C). To further confirm these observations, we seeded BMMs on bone slices in osteoclast induction medium for 3 days, followed by incubation with OEA, and then stained for actin cytoskeleton (Fig. 3B). The percentage of mature polykaryons having actin rings is significantly attenuated in the presence of OEA (Fig. 3D).

To explore whether OEA-mediated cytoskeletal alterations in osteoclasts affect bone resorption, we performed bone resorption assays and analyzed the extent of resorption pit formation using WGA staining (Fig. 3E). Consistent with its inhibitory effect on cytoskeletal organization, OEA suppresses resorption pit formation (Figs. 3E and 3F).

Osteoclast cytoskeletal organization is controlled by small GTPases whose activity is in turn regulated by M-CSF or RANKL. Given that OEA inhibits osteoclast cytoskeleton, we measured Rac activation using a Rac-GST pull-down assay. As shown in Fig. 3G, OEA strongly decreases Rac activity stimulated by M-CSF plus RANKL. We then measured Rac activity in vehicle- and OEA-treated pre-osteoclasts stimulated with either RANKL or M-CSF. Although OEA does not alter RANKL-stimulated Rac activity (Fig. 3H), it specifically blocks M-CSF-induced Rac activation (Fig. 3I).

GPR119 knockdown reverses OEA-mediated disruption of the osteoclast cytoskeleton

To determine if the effect of OEA on the osteoclast cytoskeleton is GPR119-dependent, we transduced BMMs with control or GPR119 shRNA. The mRNA expression level of GPR119 is notably reduced in GPR119 shRNA-infected cells (Fig. 4A). We then explored the effect of GPR119 knockdown on OEA-mediated inhibition of osteoclast spreading. Although OEA treatment in control shRNA-transduced cells still arrests osteoclast spreading, GPR119 knockdown significantly abrogates the OEA-mediated disruption of the osteoclast cytoskeleton (Figs. 4B and 4C). These data indicate that the OEA-induced cytoskeletal dysfunction is exerted through GPR119.

OEA promotes osteoclast apoptosis independent of GPR119

Osteoclast precursor cell proliferation and apoptosis of mature osteoclasts are important events in the regulation of osteoclast formation and resorptive function. To define the effect of OEA on precursor cell proliferation, we incubated BMMs with increasing concentrations of OEA in the presence of M-CSF and measured BrdU incorporation. OEA at 25 or 50 μM modestly increases M-CSF-induced BMM proliferation (Fig. 5A). When BMMs were incubated in culture medium containing M-CSF and RANKL for 3 days, the pro-proliferative effect of OEA is abolished (Fig. 5B).

We then assessed the impact of OEA on apoptosis in mature osteoclasts. Fully differentiated polykaryons were incubated in the absence or presence of OEA (50 and 100 μM) for 24 h and then subjected to TRAP staining (Fig. 5C). OEA sharply decreases the survival percentage of TRAP-expressing osteoclasts at both concentrations (Fig. 5D). To determine if the OEA-mediated decrease in osteoclast survival is due to accelerated apoptosis, we detected cell death using an ELISA assay. As shown in Fig. 5E, OEA significantly increases osteoclast apoptosis. Consistent with this observation, OEA accelerates caspase 3 activity and enhances the quantity of the B-cell lymphoma 2 (Bcl-2) family protein Bim, which is known to modulate osteoclast apoptosis (Fig. 5F). Given that M-CSF-stimulated ERK activity enhances cell survival via downregulation of Bim protein content, we assessed the

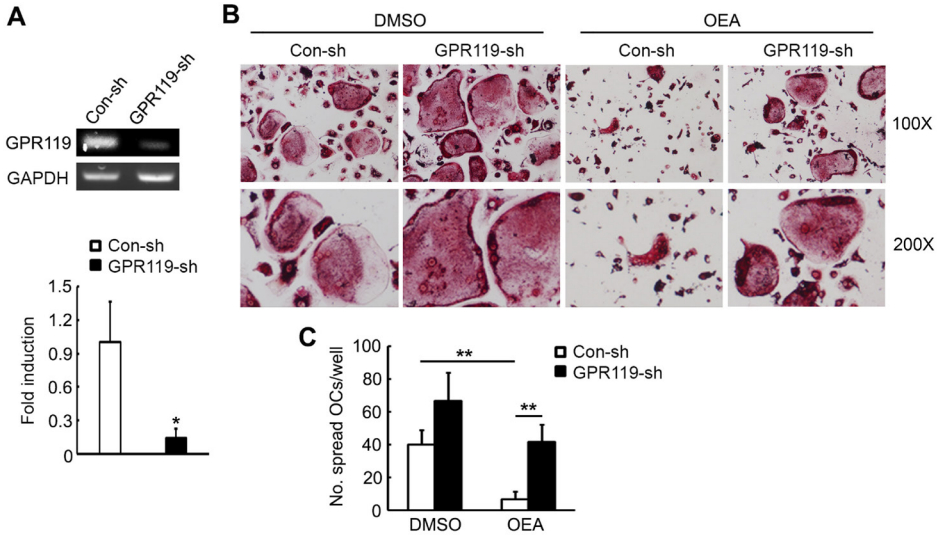

Fig. 4. GPR119 knockdown restores OEA-mediated disruption of osteoclast cytoskeleton. BMMs were transduced with scrambled control (Con-sh) or GPR119-shRNA (GPR119-sh). (A) The expression of GPR119 was analyzed using RT-PCR (upper panel) or real-time PCR (lower panel). $*P < 0.05$. (B and C) BMMs transduced with control or GPR119-shRNA were cultured with M-CSF and RANKL for 3 days. The cells were then maintained with or without OEA (50 μM) for 2 days in osteoclastogenic medium. (B) The cells were subjected to TRAP staining. Magnification, 100× (upper panel) and 200× (lower panel). (C) The number of spread osteoclasts (OCs) was counted. $**P < 0.001$.

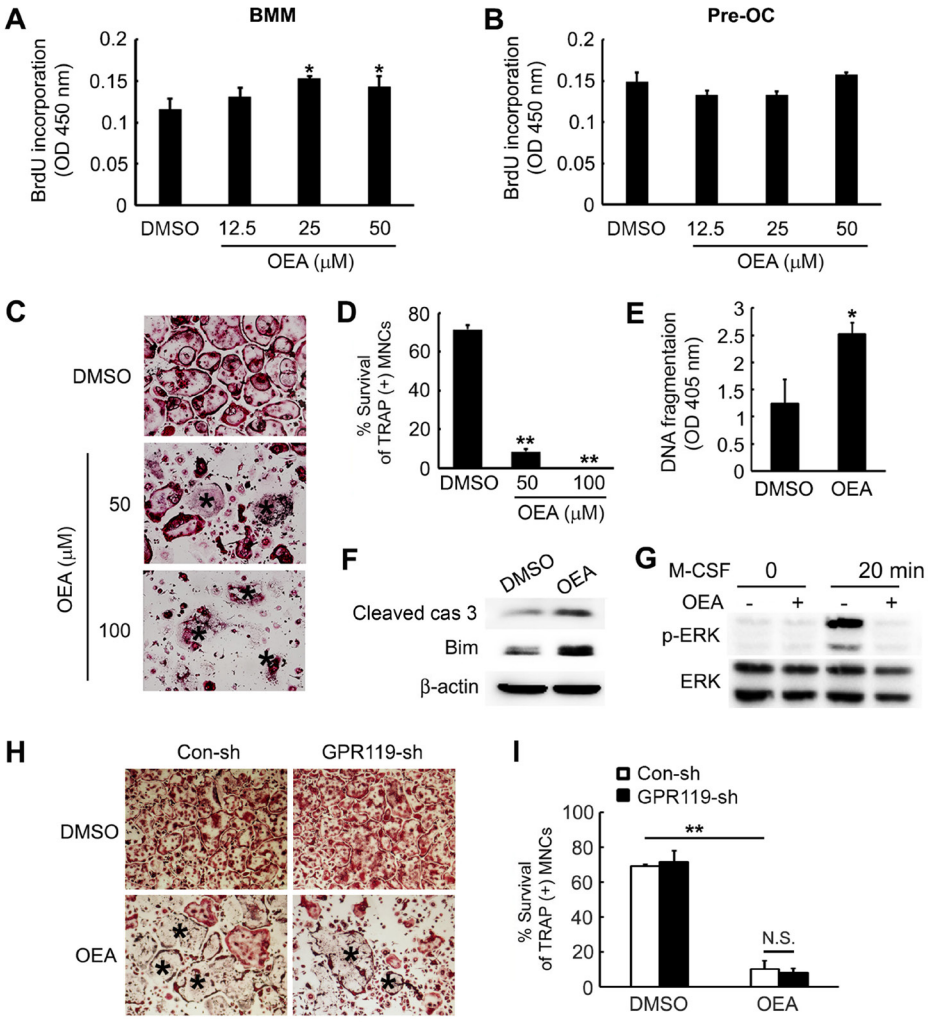

Fig. 5. OEA accelerates apoptosis in mature osteoclasts independent of GPR119. BMMs were cultured with M-CSF (30 ng/ml) in the absence (A) or presence (B) of RANKL (20 ng/ml) with the indicated concentrations of OEA. After 3 days, proliferation was determined using the BrdU incorporation assay. (C-F) Mature osteoclasts were incubated with vehicle (DMSO) or OEA for 24 h. (C) The cells were then stained for TRAP (magnification, 100×). Apoptotic osteoclasts are indicated with asterisks. (D) The survival percentage for TRAP-positive multinucleated cells (MNCs) shown in Fig. 5C was calculated. $**P < 0.001$ vs the vehicle-treated control cells. (E) The extent of apoptosis was measured using ELISA. $*P < 0.05$. (F) Cell lysates were immunoblotted with antibodies specific for cleaved caspase (cas) 3 and Bim. β-Actin served as a loading control. (G) Cytokine-starved osteoclasts were treated with OEA (50 μM) or vehicle for 16 h and then exposed to M-CSF (50 ng/ml) for 5 min. Total cell lysates were immunoblotted with an antibody specific for phosphorylated-ERK. Total ERK served as a loading control. (H) BMMs transduced with control or GPR119-shRNA were differentiated into osteoclasts in M-CSF and RANKL. The mature osteoclasts were treated with or without OEA (50 μM) for 24 h and then stained for TRAP (magnification, 40×). (I) The survival percentage for TRAP-positive MNCs shown in Fig. 5H was calculated. $**P < 0.001$. N.S., not significant.

effect of OEA on ERK signaling in response to M-CSF. OEA markedly inhibits M-CSF-induced ERK phosphorylation (Fig. 5G). We then determined whether OEA induces osteoclast apoptosis through GPR119. OEA accelerates apoptotic cell death in both control and GPR119 shRNA-transduced osteoclasts (Figs. 5H and 5I). These data imply that the pro-apoptotic function of OEA is independent of GPR119.

DISCUSSION

Fatty acids and their derivatives function as important regulators in a variety of metabolic processes. In the context of skeletal metabolism, several members of the FAA family, such as OEA, oleoyl serine, arachidonoyl ethanolamide (anandamide), and stearoyl ethanolamide, are reported to be present in trabecular bone, and some FAAs have been implicated in the modulation of skeletal remodeling and homeostasis (Smoum et al., 2010). Furthermore, previous studies revealed

that the receptors for these FAA are detected in bone tissues. For instance, cannabinoid receptors and the anandamide receptor transient receptor potential vanilloid 1 (TRPV1) have been found in osteoblasts and osteoclasts (Idris et al., 2005; 2009; Ofek et al., 2006; Rossi et al., 2009; Tam et al., 2006). GPR55 expression, known to be targeted by endogenous cannabinoids, has also been demonstrated in murine and human osteoblasts and osteoclasts (Whyte et al., 2009). GPR119, which was previously deorphanized when it was confirmed to be an OEA receptor, is expressed in osteoclast lineage cells (Kim et al., 2019b). In the current study, we explored the impact of OEA (an endogenous GPR119 ligand) on osteoclast development and observed that it regulates osteoclast cytoskeletal organization through GPR119. Therefore, our study provides an additional layer of evidence that FAA influences bone-resorbing cells through GPR119.

The number of osteoclasts in bone depends on the rates of proliferation, fusion, or differentiation of osteoclast precursor cells. We observed that OEA does not significantly impact precursor proliferation, as assessed using the BrdU and MTS assays. OEA treatment also does not affect cell-to-cell fusion, as determined by the unaltered numbers of nuclei and the similar expression levels of fusion markers, including Atp6v0d2, DC-STAMP, and OC-STAMP. In addition, RANKL-induced osteoclast differentiation was not affected by the presence of OEA.

Having established that OEA does not alter osteoclast differentiation or fusion, we then investigated its impact on osteoclast morphology. Indeed, we found that OEA-exposed osteoclasts exhibit a profound effect on cell spreading, yielding small, TRAP-expressing, multinuclear cells. The morphology of OEA-treated osteoclasts is similar to that of osteoclasts in which cytoskeleton regulating molecules have been deleted (Croke et al., 2011; McHugh et al., 2000; Reeve et al., 2009; Zou et al., 2007; 2010). For instance, mice lacking β3 integrin display an osteopetrotic phenotype owing to impaired osteoclast spreading and sealing zone formation, resulting in a lack of bone resorption (McHugh et al., 2000). Moreover, these findings are in agreement with our previous observations that impaired spreading in osteoclasts mirrors osteoclast cytoskeleton disorganization (Hong et al., 2011; Kim et al., 2006; 2014; 2016). Further examination of the suppressive role of OEA in osteoclast cytoskeletal function showed that OEA blocks the formation of actin rings and consequently inhibits resorption pit formation. Moreover, a previous study demonstrated that in the human colon carcinoma cell line Caco-2, OEA treatment caused F-actin to have an irregular morphology (Karwad et al., 2017), confirming that OEA induces cytoskeletal changes. Collectively, our findings reveal that OEA suppresses bone resorption by disrupting the osteoclast cytoskeleton.

The small GTPase Rac is known to regulate cytoskeletal organization in osteoclasts. Among Rac isoforms, Rac1 and Rac2 are expressed in osteoclasts. The key role of Rac in bone resorption by osteoclasts is demonstrated by *in vivo* studies using Rac-deficient mice. Combined deletion of Rac1 and Rac2 in bone-resorbing cells attenuates cytoskeletal organization and resorptive efficiency, yielding a severe osteopetrotic phenotype (Croke et al., 2011). Rac is activated by either M-CSF or RANKL. In this study, we observed that OEA inhibits Rac activity induced by M-CSF, but not RANKL. These findings demonstrate that OEA inhibits cytoskeletal organization in a cytokine-specific fashion. The detailed molecular mechanism by which the OEA-GPR119 axis regulates osteoclast cytoskeleton requires further investigation.

The magnitude of osteoclastic resorption is also governed by the rate of survival of mature osteoclasts as well as their precursors. Apoptosis of mature osteoclasts is associated with increased expression of Bim, a pro-apoptotic Bcl-2 protein (Akiyama et al., 2003). M-CSF is a pro-survival cytokine, and M-CSF-induced ERK activation accelerates ubiquitination-dependent Bim degradation, thereby promoting osteoclast survival. Hence, osteoclasts that are differentiated from BMMs of Bim-deficient mice show increased cell survival in the absence of M-CSF (Akiyama et al., 2003). We also found that OEA promotes osteoclast apoptosis by increasing the level of Bim protein. Furthermore, M-CSF-induced ERK activation was completely abrogated in the presence of OEA. Conversely, BMM viability was unaffected by OEA treatment, as determined by the MTS assay, suggesting that OEA may not be involved in the modulation of osteoclast precursor survival.

This study also shows that OEA is a non-specific GPR119 agonist in terms of osteoclast apoptosis. The pro-apoptotic effect of OEA was not restored by GPR119 knockdown, indicating that OEA-induced acceleration of osteoclast apoptosis is GPR119-independent. Likewise, a previous study reported that cell death in astrocytoma brain tumors was induced by OEA via TRPV1 (Stock et al., 2012), but not GPR119. Because OEA also functions as a TRPV1 agonist, we speculate that OEA might promote osteoclast apoptosis through TRPV1.

In conclusion, our study demonstrates that a bioactive lipid, OEA, suppresses osteoclast cytoskeletal organization through GPR119. Mechanistically, OEA inhibits M-CSF-stimulated Rac

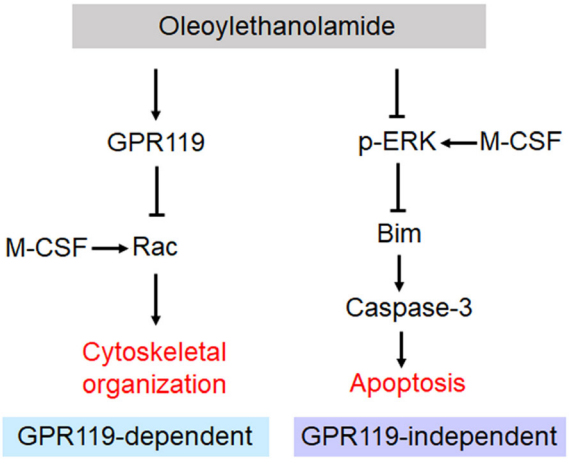

Fig. 6. Schematic model for OEA in osteoclast function and survival. OEA suppresses osteoclast cytoskeletal organization in a GPR119-dependent manner by inhibiting M-CSF-induced Rac activity (left arm). In addition, OEA accelerates osteoclast apoptosis independent of GPR119 by suppressing M-CSF-induced ERK activation and inducing Bim expression (right arm).

activity, which is important for osteoclast cytoskeletal organization and bone resorption. OEA also induces apoptosis in mature osteoclasts independent of GPR119 by suppressing M-CSF-mediated ERK activation and increasing Bim expression (Fig. 6). Therefore, we propose that OEA is a candidate target for the development of therapeutic strategies in skeletal diseases that involve excessive osteoclast activity.

Disclosure

The authors have no potential conflicts of interest to disclose.

ACKNOWLEDGMENTS

This work was supported by the National Research Foundation of Korea (NRF) grant funded by the Korea Government (MSIT) (No. 2018R1A2B6001298, No. 2017R1A5A2015391); and the Bio & Medical Technology Development Program (NRF-2017M3A9G8083382).

ORCID

Hyun-Ju Kim https://orcid.org/0000-0002-5836-5841
Dong-Kyo Lee https://orcid.org/0000-0002-5202-5352
Xian Jin https://orcid.org/0000-0002-8273-0108
Xiangguo Che https://orcid.org/0000-0002-7272-1806
Je-Yong Choi https://orcid.org/0000-0002-5057-8842

REFERENCES

Akiyama, T., Bouillet, P., Miyazaki, T., Kadono, Y., Chikuda, H., Chung, U.I., Fukuda, A., Hikita, A., Seto, H., Okada, T., et al. (2003). Regulation of osteoclast apoptosis by ubiquitylation of proapoptotic BH3-only Bcl-2 family member Bim. EMBO J. *22*, 6653-6664.

Boyle, W.J., Simonet, W.S., and Lacey, D.L. (2003). Osteoclast differentiation and activation. Nature *423*, 337-342.

Chellaiah, M.A., Soga, N., Swanson, S., McAllister, S., Alvarez, U., Wang, D., Dowdy, S.F., and Hruska, K.A. (2000). Rho-A is critical for osteoclast podosome organization, motility, and bone resorption. J. Biol. Chem. *275*, 11993-12002.

Croke, M., Ross, F.P., Korhonen, M., Williams, D.A., Zou, W., and Teitelbaum, S.L. (2011). Rac deletion in osteoclasts causes severe osteopetrosis. J. Cell Sci. *124*, 3811-3821.

Di Paola, M., Bonechi, E., Provensi, G., Costa, A., Clarke, G., Ballerini, C., De Filippo, C., and Passani, M.B. (2018). Oleoylethanolamide treatment affects gut microbiota composition and the expression of intestinal cytokines in Peyer's patches of mice. Sci. Rep. *8*, 14881.

Faccio, R., Teitelbaum, S.L., Fujikawa, K., Chappel, J., Zallone, A., Tybulewicz, V.L., Ross, F.P., and Swat, W. (2005). Vav3 regulates osteoclast function and bone mass. Nat. Med. *11*, 284-290.

Fu, J., Gaetani, S., Oveisi, F., Lo Verme, J., Serrano, A., Rodriguez De Fonseca, F., Rosengarth, A., Luecke, H., Di Giacomo, B., Tarzia, G., et al. (2003). Oleylethanolamide regulates feeding and body weight through activation of the nuclear receptor PPAR-alpha. Nature *425*, 90-93.

Hong, J.M., Teitelbaum, S.L., Kim, T.H., Ross, F.P., Kim, S.Y., and Kim, H.J. (2011). Calpain-6, a target molecule of glucocorticoids, regulates osteoclastic bone resorption via cytoskeletal organization and microtubule acetylation. J. Bone Miner. Res. *26*, 657-665.

Idris, A.I., Sophocleous, A., Landao-Bassonga, E., Canals, M., Milligan, G., Baker, D., van't Hof, R.J., and Ralston, S.H. (2009). Cannabinoid receptor type 1 protects against age-related osteoporosis by regulating osteoblast and adipocyte differentiation in marrow stromal cells. Cell Metab. *10*, 139-147.

Idris, A.I., van't Hof, R.J., Greig, I.R., Ridge, S.A., Baker, D., Ross, R.A., and Ralston, S.H. (2005). Regulation of bone mass, bone loss and osteoclast activity by cannabinoid receptors. Nat. Med. *11*, 774-779.

Ito, Y., Teitelbaum, S.L., Zou, W., Zheng, Y., Johnson, J.F., Chappel, J., Ross, F.P., and Zhao, H. (2010). Cdc42 regulates bone modeling and remodeling in mice by modulating RANKL/M-CSF signaling and osteoclast polarization. J. Clin. Invest. *120*, 1981-1993.

Itokowa, T., Zhu, M.L., Troiano, N., Bian, J., Kawano, T., and Insogna, K. (2011). Osteoclasts lacking Rac2 have defective chemotaxis and resorptive activity. Calcif. Tissue Int. *88*, 75-86.

Itzstein, C., Coxon, F.P., and Rogers, M.J. (2011). The regulation of osteoclast function and bone resorption by small GTPases. Small GTPases *2*, 117-130.

Karwad, M.A., Macpherson, T., Wang, B., Theophilidou, E., Sarmad, S., Barrett, D.A., Larvin, M., Wright, K.L., Lund, J.N., and O'Sullivan, S.E. (2017). Oleoylethanolamine and palmitoylethanolamine modulate intestinal permeability in vitro via TRPV1 and PPARalpha. FASEB J. *31*, 469-481.

Kim, H.J., Kim, B.K., Ohk, B., Yoon, H.J., Kang, W.Y., Cho, S., Seong, S.J., Lee, H.W., and Yoon, Y.R. (2019a). Estrogen-related receptor gamma negatively regulates osteoclastogenesis and protects against inflammatory bone loss. J. Cell. Physiol. *234*, 1659-1670.

Kim, H.J., Yoon, H.J., Choi, J.Y., Lee, I.K., and Kim, S.Y. (2014). The tyrosine kinase inhibitor GNF-2 suppresses osteoclast formation and activity. J. Leukoc. Biol. *95*, 337-345.

Kim, H.J., Yoon, H.J., Kim, B.K., Kang, W.Y., Seong, S.J., Lim, M.S., Kim, S.Y., and Yoon, Y.R. (2016). G protein-coupled receptor 120 signaling negatively regulates osteoclast differentiation, survival, and function. J. Cell. Physiol. *231*, 844-851.

Kim, H.J., Yoon, H.J., Park, J.W., Che, X., Jin, X., and Choi, J.Y. (2019b). G protein-coupled receptor 119 is involved in RANKL-induced osteoclast differentiation and fusion. J. Cell. Physiol. *234*, 11490-11499.

Kim, H.J., Zhao, H., Kitaura, H., Bhattacharyya, S., Brewer, J.A., Muglia, L.J., Ross, F.P., and Teitelbaum, S.L. (2006). Glucocorticoids suppress bone formation via the osteoclast. J. Clin. Invest. *116*, 2152-2160.

Kim, M.K., Kim, B., Kwon, J.O., Song, M.K., Jung, S., Lee, Z.H., and Kim, H.H. (2019c). ST5 positively regulates osteoclastogenesis via Src/Syk/calcium signaling pathways. Mol. Cells *42*, 810-819.

Kong, Y.Y., Yoshida, H., Sarosi, I., Tan, H.L., Timms, E., Capparelli, C., Morony, S., Oliveira-dos-Santos, A.J., Van, G., Itie, A., et al. (1999). OPGL is a key regulator of osteoclastogenesis, lymphocyte development and lymph-node organogenesis. Nature *397*, 315-323.

Lacey, D.L., Timms, E., Tan, H.L., Kelley, M.J., Dunstan, C.R., Burgess, T., Elliott, R., Colombero, A., Elliott, G., Scully, S., et al. (1998). Osteoprotegerin ligand is a cytokine that regulates osteoclast differentiation and activation. Cell *93*, 165-176.

Lauffer, L.M., Iakoubov, R., and Brubaker, P.L. (2009). GPR119 is essential for oleoylethanolamide-induced glucagon-like peptide-1 secretion from the intestinal enteroendocrine L-cell. Diabetes *58*, 1058-1066.

McHugh, K.P., Hodivala-Dilke, K., Zheng, M.H., Namba, N., Lam, J., Novack, D., Feng, X., Ross, F.P., Hynes, R.O., and Teitelbaum, S.L. (2000). Mice lacking beta3 integrins are osteosclerotic because of dysfunctional osteoclasts. J. Clin. Invest. *105*, 433-440.

McKillop, A.M., Moran, B.M., Abdel-Wahab, Y.H., Gormley, N.M., and Flatt, P.R. (2016). Metabolic effects of orally administered small-molecule agonists of GPR55 and GPR119 in multiple low-dose streptozotocin-induced diabetic and incretin-receptor-knockout mice. Diabetologia *59*, 2674-2685.

Ofek, O., Karsak, M., Leclerc, N., Fogel, M., Frenkel, B., Wright, K., Tam, J., Attar-Namdar, M., Kram, V., Shohami, E., et al. (2006). Peripheral cannabinoid receptor, CB2, regulates bone mass. Proc. Natl. Acad. Sci. U. S. A. *103*, 696-701.

Overton, H.A., Babbs, A.J., Doel, S.M., Fyfe, M.C., Gardner, L.S., Griffin,

G., Jackson, H.C., Procter, M.J., Rasamison, C.M., Tang-Christensen, M., et al. (2006). Deorphanization of a G protein-coupled receptor for oleoylethanolamide and its use in the discovery of small-molecule hypophagic agents. Cell Metab. *3*, 167-175.

Provensi, G., Coccurello, R., Umehara, H., Munari, L., Giacovazzo, G., Galeotti, N., Nosi, D., Gaetani, S., Romano, A., Moles, A., et al. (2014). Satiety factor oleoylethanolamide recruits the brain histaminergic system to inhibit food intake. Proc. Natl. Acad. Sci. U. S. A. *111*, 11527-11532.

Reeve, J.L., Zou, W., Liu, Y., Maltzman, J.S., Ross, F.P., and Teitelbaum, S.L. (2009). SLP-76 couples Syk to the osteoclast cytoskeleton. J. Immunol. *183*, 1804-1812.

Rodriguez de Fonseca, F., Navarro, M., Gomez, R., Escuredo, L., Nava, F., Fu, J., Murillo-Rodriguez, E., Giuffrida, A., LoVerme, J., Gaetani, S., et al. (2001). An anorexic lipid mediator regulated by feeding. Nature *414*, 209-212.

Rossi, F., Siniscalco, D., Luongo, L., De Petrocellis, L., Bellini, G., Petrosino, S., Torella, M., Santoro, C., Nobili, B., Perrotta, S., et al. (2009). The endovanilloid/endocannabinoid system in human osteoclasts: possible involvement in bone formation and resorption. Bone *44*, 476-484.

Smoum, R., Bar, A., Tan, B., Milman, G., Attar-Namdar, M., Ofek, O., Stuart, J.M., Bajayo, A., Tam, J., Kram, V., et al. (2010). Oleoyl serine, an endogenous N-acyl amide, modulates bone remodeling and mass. Proc. Natl. Acad. Sci. U. S. A. *107*, 17710-17715.

Stock, K., Kumar, J., Synowitz, M., Petrosino, S., Imperatore, R., Smith, E.S., Wend, P., Purfurst, B., Nuber, U.A., Gurok, U., et al. (2012). Neural precursor cells induce cell death of high-grade astrocytomas through stimulation of TRPV1. Nat. Med. *18*, 1232-1238.

Takayanagi, H. (2007). Osteoimmunology: shared mechanisms and crosstalk between the immune and bone systems. Nat. Rev. Immunol. *7*, 292-304.

Takeshita, S., Kaji, K., and Kudo, A. (2000). Identification and characterization of the new osteoclast progenitor with macrophage phenotypes being able to differentiate into mature osteoclasts. J. Bone Miner. Res. *15*, 1477-1488.

Tam, J., Ofek, O., Fride, E., Ledent, C., Gabet, Y., Muller, R., Zimmer, A., Mackie, K., Mechoulam, R., Shohami, E., et al. (2006). Involvement of neuronal cannabinoid receptor CB1 in regulation of bone mass and bone remodeling. Mol. Pharmacol. *70*, 786-792.

Teitelbaum, S.L. (2000). Bone resorption by osteoclasts. Science *289*, 1504-1508.

Touaitahuata, H., Blangy, A., and Vives, V. (2014). Modulation of osteoclast differentiation and bone resorption by Rho GTPases. Small GTPases *5*, e28119.

Vives, V., Laurin, M., Cres, G., Larrousse, P., Morichaud, Z., Noel, D., Cote, J.F., and Blangy, A. (2011). The Rac1 exchange factor Dock5 is essential for bone resorption by osteoclasts. J. Bone Miner. Res. *26*, 1099-1110.

Whyte, L.S., Ryberg, E., Sims, N.A., Ridge, S.A., Mackie, K., Greasley, P.J., Ross, R.A., and Rogers, M.J. (2009). The putative cannabinoid receptor GPR55 affects osteoclast function in vitro and bone mass in vivo. Proc. Natl. Acad. Sci. U. S. A. *106*, 16511-16516.

Wong, B.R., Josien, R., Lee, S.Y., Sauter, B., Li, H.L., Steinman, R.M., and Choi, Y. (1997). TRANCE (tumor necrosis factor [TNF]-related activation-induced cytokine), a new TNF family member predominantly expressed in T cells, is a dendritic cell-specific survival factor. J. Exp. Med. *186*, 2075-2080.

Yasuda, H., Shima, N., Nakagawa, N., Yamaguchi, K., Kinosaki, M., Mochizuki, S., Tomoyasu, A., Yano, K., Goto, M., Murakami, A., et al. (1998). Osteoclast differentiation factor is a ligand for osteoprotegerin/osteoclastogenesis-inhibitory factor and is identical to TRANCE/RANKL. Proc. Natl. Acad. Sci. U. S. A. *95*, 3597-3602.

Zou, W., Kitaura, H., Reeve, J., Long, F., Tybulewicz, V.L., Shattil, S.J., Ginsberg, M.H., Ross, F.P., and Teitelbaum, S.L. (2007). Syk, c-Src, the alphavbeta3 integrin, and ITAM immunoreceptors, in concert, regulate osteoclastic bone resorption. J. Cell Biol. *176*, 877-888.

Zou, W., Zhu, T., Craft, C.S., Broekelmann, T.J., Mecham, R.P., and Teitelbaum, S.L. (2010). Cytoskeletal dysfunction dominates in DAP12-deficient osteoclasts. J. Cell Sci. *123*, 2955-2963.